EPR Spectroscopy of MRI-Related Gd(III) Complexes: Simultaneous Analysis of Multiple Frequency and Temperature Spectra, Including Static and Transient Crystal Field Effects

Sebastian Rast,[†] Alain Borel,[†] Lothar Helm,[†] Elie Belorizky,[‡] Pascal H. Fries,*[,§] and André E. Merbach*[,†]

Contribution from the Institut de Chimie Minérale et Analytique, Université de Lausanne, CH-1015 Lausanne, Switzerland, the Laboratoire de Spectrométrie Physique, CNRS-UMR 5588, Université Joseph Fourier, BP 87, F-38402 Saint-Martin d'Hères Cédex, France, and the Laboratoire de Reconnaissance Ionique, Service de Chimie Inorganique et Biologique (UMR 5046), Département de Recherche Fondamentale sur la Matière Condensée, CEA-Grenoble, F-38054 Grenoble Cédex 9, France

Received October 17, 2000. Revised Manuscript Received January 5, 2001

Abstract: For the first time, a very general theoretical method is proposed to interpret the full electron paramagnetic resonance (EPR) spectra at multiple temperatures and frequencies in the important case of *S*-state metal ions complexed in liquid solution. This method is illustrated by a careful analysis of the measured spectra of two Gd^{3+} ($S = {}^7/_2$) complexes. It is shown that the electronic relaxation mechanisms at the origin of the EPR line shape arise from the combined effects of the modulation of the static crystal field by the random Brownian rotation of the complex and of the transient zero-field splitting. A detailed study of the static crystal field mechanism shows that, contrarily to the usual global models involving only second-order terms, the fourth and sixth order terms can play a non-negligible role. The obtained parameters are well interpreted in the framework of the physics of the various underlying relaxation processes. A better understanding of these mechanisms is highly valuable since they partly control the efficiency of paramagnetic metal ions in contrast agents for medical magnetic resonance imaging (MRI).

1. Introduction

Paramagnetic ($S = {}^7/_2$) Gd^{3+} complexes are widely used as contrast agents in magnetic resonance imaging (MRI) due to their enhancement of the relaxation of the neighboring protons.[1] This relaxation rate enhancement, the so-called *relaxivity*, is a consequence of the dipolar coupling between the proton nuclear spin and the electronic spin of the metal ion. The relaxivity is usually divided into an inner-sphere contribution coming from the water molecules directly bound to the metal ion, and an outer-sphere contribution stemming from the bulk water protons. The inner-sphere contribution is determined by (1) the rotational correlation time of the complex τ_R, (2) the water residence time τ_M in the first coordination shell, and (3) the electronic spin relaxation. The outer-sphere relaxivity is mainly governed by translational diffusion but is also influenced by the electronic spin relaxation. While (1) and (2) are rather well understood,[1] the electronic spin relaxation theory still needs an improvement to be included in a complete description of the magnetic resonance experiments on Gd^{3+} complexes relevant for MRI.[2−6] The influence of the electronic spin relaxation on the relaxivity is essentially governed by the decay of the electronic spin magnetization in the direction parallel to the external field. This decay is described by the longitudinal electronic relaxation time T_{1e} of the Gd^{3+} complexes which is too short for being directly measurable by the presently available techniques. Nevertheless, the investigation of the decay of the electronic spin magnetization perpendicular to the external field, usually characterized by a transverse electronic relaxation time T_{2e}, may allow an estimation of T_{1e} within the framework of a given model of the electronic relaxation. For a reasonable prediction of T_{1e}, we need to find a model which correctly describes the underlying physics. For this purpose, multiple frequency and temperature EPR measurements were performed to get detailed information about the dynamics of the system.

The basic theory of the EPR line shape of Gd^{3+} complexes was proposed three decades ago by Hudson and Lewis.[7] A transient zero-field splitting was used as the main relaxation mechanism. The transverse electronic spin relaxation could not be described by a single T_{2e}, but four different relaxation times were necessary as the experimental spectrum results from a superposition of four transitions with different intensities. To simplify this theory, Powell et al.[2] proposed empirical formulas to describe both the transverse and longitudinal relaxation times, which they later applied in a unified model to simultaneously interpret ^{17}O NMR, ^1H NMR, and EPR.[3,8] However, they found it necessary to add a spin rotation mechanism in their interpreta-

* Authors for correspondence. E-mail: fries@drfmc.ceng.cea.fr. E-mail: andre.merbach@icma.unil.ch..

‡ Université Joseph Fourier.

§ CEA-Grenoble.

† Université de Lausanne.

(1) Caravan, P.; Ellison, J. J.; McMurry, T. J.; Lauffer, R. B. *Chem. Rev.* **1999**, *99*, 2293.

(2) Powell, D. H.; Merbach, A. E.; González, G.; Brücher, E.; Micskei, K.; Ottaviani, M. F.; Köhler, K.; von Zelewsky, A.; Grinberg, O. Ya.; Lebedev, Ya. S. *Helv. Chim. Acta* **1993**, *76*, 2129.

(3) Powell, D. H.; Ni Dhubhghaill, O. M.; Pubanz, D.; Helm, L.; Lebedev, Ya. S.; Schlaepfer, W.; Merbach, A. E. *J. Am. Chem. Soc.* **1996**, *118*, 9333.

(4) Clarkson, R. B.; Smirnov, A. I.; Smirnova, T. I.; Kang, H.; Belford, R. L.; Earle, K.; Freed, J. H. *Mol. Phys.* **1998**, *95*, 1325.

(5) Borel, A.; Tóth, É.; Helm, L.; Jánossy, A.; Merbach, A. E. *PCCP* **2000**, *2*, 1311.

(6) *Rare-Earth Information Center News* **1999**, *2*, 4.

(7) Hudson, A.; Lewis, J. W. E. *Trans. Faraday Soc.* **1970**, *66*, 1297.

10.1021/ja003707u CCC: $20.00
Published on Web 02/24/2001

tion of the measurements. Even so, the obtained results were in a generally poor agreement with the experimental EPR data.

More recent approaches also account for the dynamic frequency shift, which is a small displacement in the transition frequencies, often neglected. Several theoretical treatments of this effect were independently proposed by different groups. Strandberg and Westlund[9] used the superoperator formalism to derive an analytical expression for the EPR line shape. This approach is equivalent to the earlier development of Poupko et al.[10] but has never been applied to the analysis of extensive experimental data sets. Although the inclusion of the dynamic shift is an improvement, the description of the crystal field dynamics remains the same as in the work of Hudson and Lewis. Clarkson and co-workers[4,11] used a theory originally developed by Alexander et al.[12] to derive simple equations for the line widths and shifts. However, these equations are only valid for high-frequency measurements. Furthermore, the dynamic shift is independent of temperature in their approximation.

The recent EPR experiments on $[Gd(H_2O)_8]^{3+}$ and $[Gd(DOTA)(H_2O)]^-$ at various temperatures and field strengths[5] represent a rich collection of full spectra including peak-to-peak distances supplemented with dynamic frequency shifts which contain valuable complementary information that is rarely published because these shifts are difficult to measure and interpret. Borel et al.[5] interpreted their data with the help of the above-mentioned model of the crystal field modulation in the framework of Redfield's relaxation theory[13a] in which they also took the frequency shift into account. This analysis, performed for the first time over such a wide temperature and frequency range, showed the shortcomings of the model. As in the work of Powell et al.,[3] a spin rotation mechanism had to be introduced to obtain a satisfactory fit of the data.

Very recently, Rast et al.[14,15] developed a refined model of the electronic relaxation of the *S* states of metal ion complexes in solutions. This refined treatment now includes the contribution of the static crystal field surrounding the Gd^{3+} ion caused by its modulation by the rotation of the whole complex besides a part due to the usual transient crystal zero-field splitting (ZFS) caused by vibration, intramolecular rearrangement, and collision with surrounding solvent molecules. A good agreement with the measured peak-to-peak distances was obtained for $[Gd(H_2O)_8]^{3+}$, $[Gd(DTPA)(H_2O)]^{2-}$, and $[Gd(DTPA\text{-}BMA)(H_2O)]$ complexes over wide ranges of magnetic fields and temperatures. But no attempt was made for the interpretation of the EPR shifts and line shapes.

The purpose of this paper is precisely to remove this lack of interpretation of the EPR spectra, and it will be shown that our model including the effects of the static crystal field and of the transient ZFS is able to provide a complete and satisfactory description of the full line shapes under all of the investigated experimental conditions. In the framework of this new model, and contrarily to previous works,[3,5] it is not necessary to include the spin rotation mechanism in the interpretation of the measurements as this effect is expected to be very weak for these large complexes.[16] Our theory is very general and can be used for all systems where the orbital angular momentum is zero as in the Fe^{3+}, Mn^{2+}, Gd^{3+}, and Eu^{2+} complexes.[17−19]

The main features of our model are described in the theoretical section. The following section is devoted to some computational details about our programs. In the last section, we present and discuss our results concerning the $[Gd(H_2O)_8]^{3+}$ and $[Gd(DOTA)(H_2O)]^-$ complexes.

2. Theory

The model described hereafter is developed in the framework of Redfield's relaxation theory, so that it is valid for weak crystal fields and fast fluctuations.[13b] The multiparticle Hamiltonian of the statistical ensemble of probe molecules in solution is replaced by a one-particle Hamiltonian approximating the spin-lattice interaction by a random time-dependent operator. The knowledge of the correlation functions of its matrix elements allows calculation of the line shape of the EPR spectra.

2.1. Crystal Field Hamiltonian. The Hamiltonian of the system is a time dependent random operator $\hbar H(t)$ containing two main contributions in the laboratory (L) frame *Oxyz*, the time-independent Zeeman term

$$\hbar H_0 = \hbar \omega_0 S_z \tag{1}$$

where ω_0 is the EPR Larmor frequency, and a time-dependent random term $\hbar H_1^{(L)}(t)$ which describes the fluctuating crystal field, the superscript (L) indicating that it is also written in the laboratory frame. The complete Hamiltonian is

$$\hbar H(t) = \hbar H_0 + \hbar H_1^{(L)}(t) \tag{2}$$

It is easier to define the crystal field Hamiltonian in the molecular (M) frame *OXYZ* and to transform it into the laboratory frame later. In the molecular frame we have a static contribution of the crystal field which we express as linear combinations of irreducible tensor operators $\mathcal{T}_k^q$($|q| \leq k$) of rank k of the electronic spin components.[20] The resulting static crystal field Hamiltonian is:

$$\hbar H_{1S}^{(M)} = \hbar \sum_{k=2}^{K} \sum_{\alpha} B_{k\alpha} \sum_{q=-k}^{k} b_{k\alpha}^q \mathcal{T}_k^q \tag{3}$$

Only even values of k are involved. For d electrons $K = 4$ and for f electrons $K = 6$. The linear combinations $\Sigma_{q=-k}^{k} b_{k\alpha}^q \mathcal{T}_k^q$ have complex coefficients $b_{k\alpha}^q$ and must be invariant under the operations of the symmetry group of the system. There are in general several such linear combinations of same rank k, making necessary the supplementary index α. The coefficients $b_{k\alpha}^q$ can always be chosen orthonormal:

$$\sum_{q=-k}^{k} (b_{k\alpha}^q)^* b_{k\alpha'}^q = \delta_{\alpha\alpha'} \tag{4}$$

The real coefficients $B_{k\alpha}$ determine the magnitude of each contribution and are time-independent. This is no more the case for the fluctuating contribution describing the variation of the crystal field due to vibrations and intramolecular rearrangements. Here, we restrict ourselves to the second-order terms obtaining

$$\hbar H_{1T}^{(M)}(t) = \hbar \sum_{\alpha} B_{2\alpha T}(t) \sum_{q=-2}^{2} b_{2\alpha T}^q \mathcal{T}_2^q \tag{5}$$

where $\mathcal{T}_2^q$ are the irreducible tensor operators of rank 2, the complex

(8) González, G.; Powell, D. H.; Tissières, V.; Merbach, A. E. *J. Phys. Chem.* **1994**, *98*, 53.
(9) Strandberg, E.; Westlund, P.-O. *J. Magn. Res. A* **1996**, *122*, 179.
(10) Poupko, R.; Baram, A.; Luz, Z. *Mol. Phys.* **1974**, *27*, 1345.
(11) Smirnova, T. I.; Smirnov, A. I.; Belford, R. L.; Clarkson, R. B. *J. Am. Chem. Soc.* **1998**, *120*, 5060.
(12) Alexander, S.; Luz, Z.; Naor, Y.; Poupko, R. *Mol. Phys.* **1977**, *33*, 1119.
(13) Abragam, A. *The Principles of Nuclear Magnetism*; Oxford University Press: New York, 1961: (a) pp 442−447, (b) p 282, (c) p 279.
(14) Rast, S.; Fries, P. H.; Belorizky, E. *J. Chem. Phys.* **2000**, *113*, 8724.
(15) Rast, S.; Fries, P. H.; Belorizky, E. *J. Chim. Phys.* **1999**, *96*, 1543.
(16) Nyberg, G. *Mol. Phys.* **1967**, *12*, 69.
(17) Sur, S. K.; Bryant, R. G. *J. Phys. Chem.* **1995**, *99*, 6301.
(18) Hinckley, C. C.; Morgan, L. O. *J. Chem. Phys.* **1966**, *44*, 898.
(19) Garrett, B. B.; Morgan, L. O. *J. Chem. Phys.* **1966**, *44*, 890.

coefficients $b^q_{2\alpha T}$ are again assumed to be orthonormal ($\Sigma^2_{q=-2}(b^q_{2\alpha T})^* b^q_{2\alpha' T} = \delta_{\alpha\alpha'}$) and $B_{2\alpha T}(t)$ are time-dependent real random functions with zero average values $\overline{B_{2\alpha T}(t)} = 0$.

The transformation of $H_1^{(M)}(t) = H_{1S}^{(M)} + H_{1T}^{(M)}(t)$ from the molecular frame into the laboratory frame is performed in the following way. Denoting by R_t the rotations transforming *Oxyz* into *OXYZ* at time *t*, and by $D^k(R_t)$ the associated active Wigner rotation matrix of rank *k* we get for $H_1^{(L)}(t)$:

$$H_1^{(L)}(t) = \sum_{k=2}^{K}\sum_{\alpha} B_{k\alpha} \sum_{q,q'=-k}^{K} b_{k\alpha}{}^{q}\, \mathcal{T}_k^{q'} D_{q'q}{}^{k}(R_t) + \sum_{\alpha} B_{2\alpha T}(t) \sum_{q,q'=-2}^{2} b^q_{2\alpha T}\, \mathcal{T}_k^{q'} D_{q'q}{}^{k}(R_t) \quad (6)$$

In the molecular frame, the best known form of these type of operators is a second rank term

$$D\left(S_z^2 - \frac{S(S+1)}{3}\right) + E(S_+^2 + S_-^2) = D\mathcal{T}_2^0 + \frac{E}{2}(\mathcal{T}_2^{-2} + \mathcal{T}_2^2) \quad (7)$$

with real coefficients *D*, *E*.

2.2. EPR Line Shape. We have built the Hamiltonian which governs the time evolution of our quantum mechanical system, and we turn our attention to the line shape. Let us consider a spin operator component S_i with $i = x,y,z$ and its correlation function

$$G_i(t) = \frac{1}{2S+1}\mathrm{tr}\overline{S_i(t)S_i(0)} \quad (8)$$

The bar indicates the mean value of the matrix elements of these operators, and tr is the trace operation. In what follows, it is useful to define a slowly time varying operator $\tilde{S}_i(t) = e^{-iH_0 t}S_i(t)e^{-iH_0 t}$, $i = x,y,z$ and the vectors $\vec{X}$, $\vec{Z}$ in a $2S$ or $2S+1$ dimensional space, the components of which are $X_M(t) = \overline{\langle M|\tilde{S}_x(t)|M-1\rangle}$, $M = -S+1, ..., S$ and $Z_M(t) = \overline{\langle M|\tilde{S}_z(t)|M\rangle}$, $M = -S, ..., S$. Defining $g_x(t)$ as

$$g_x(t) = \frac{1}{2S+1}\sum_{M=-S+1}^{S} e^{i\omega_0 t} X_M(t)X_M(0) \quad (9)$$

we have shown[14] that, at constant external magnetic field B_0 corresponding to a resonance frequency $\omega_0 = g\mu_B B_0/\hbar$ and variable frequency ω, the measured EPR absorption line shape is proportional to the derivative of the Fourier transform of

$$G_x(t) = \begin{cases} g_x(t) + g_x(t)^* & t \geq 0 \\ g_x(-t) + g_x(-t)^* & t < 0 \end{cases} \quad (10)$$

From eq 9 we have to calculate $X_M(t) = \overline{\langle M|\tilde{S}_x(t)|M-1\rangle}$. For this purpose, we use Redfield's approximation which gives these matrix elements as a solution of a system of linear differential equations[14]

$$\frac{dX_M}{dt} = \sum_{M_1} R_{MM-1,M_1M_1-1}(-\omega_0)X_{M_1} \quad (11)$$

where $R_{MM-1,M_1M_1-1}(-\omega_0)$ are constant matrix elements of the so-called Redfield relaxation matrix. The matrix elements $R_{MM',M_1M_1'}$ are linear combinations written in terms of the spectral densities $j_{MM',M_1M_1'}(\omega)$ and are defined by the general eqs 8 and 4 of reference 14. The initial condition for the system of equations (11) is $X_M(0) = \langle M|S_x|M-1\rangle = \sqrt{S(S+1)-M(M-1)}/2$.

Similarly, the longitudinal relaxation behavior is described by

$$G_z(t) = \frac{1}{2S+1}\sum_{M=-S}^{S} Z_M(t)Z_M(0) \quad (12)$$

where the matrix elements $Z_M(t)$ satisfy:

$$\frac{dZ_M}{dt} = \sum_{M_1} R_{MM,M_1M_1}(-\omega_0)Z_{M_1} \quad (13)$$

with the initial condition $Z_M(0) = \langle M|S_z(t)|M\rangle = M$.

Generally, the spectral densities are complex functions, and therefore the matrix $R_{MM',M_1M_1'}$ is also complex. It has been shown[14,21] that the relevant Redfield matrix for the transverse relaxation $A^X_{MM_1} = R_{MM-1,M_1M_1-1}$ is complex and symmetric (but is not a normal matrix) leading to complex eigenvalues. On the other hand, the relevant matrix $A^Z_{MM_1} = R_{MM,M_1M_1}$ for the longitudinal relaxation is a real symmetric matrix. The technical details concerning the diagonalization of these matrices are discussed in the Computational Details section. In our case we have checked that the eigenspace of $A^X_{MM_1}(-\omega_0) = R_{MM-1,M_1M_1-1}(-\omega_0)$ ($M, M_1 = -S+1, ..., S$) is $2S$-dimensional and its eigenvalues are denoted by Λ_M, $M = -S+1, ..., S$ with the corresponding eigenvectors $\vec{\eta}_M$, $M = -S+1, ..., S$ which have to be chosen to fulfill the relation $\Sigma^S_{\mu=-S+1}\eta_{M,\mu}\eta_{M'\mu} = \delta_{MM'}$. At a given external magnetic field B_0 with an associated frequency ω_0, we obtain an explicit formula for the Fourier transform of $G_x(t)$ which is denoted by $\hat{G}_x(\omega,\omega_0)$.[10] For $\omega \approx \omega_0$ this Fourier transform can be safely approximated as:

$$\hat{G}_x(\omega,\omega_0) \approx \sum_{M=-S+1}^{S}\left\{\frac{\mathrm{Re}[(\vec{X}(0),\vec{\eta}_M)^2]\mathrm{Re}\Lambda_M}{[\omega-(\omega_0+\mathrm{Im}\Lambda_M)]^2+(\mathrm{Re}\Lambda_M)^2} - \frac{\mathrm{Im}[(\vec{X}(0),\vec{\eta}_M)^2][\omega-(\omega_0+\mathrm{Im}\Lambda_M)]}{[\omega-(\omega_0+\mathrm{Im}\Lambda_M)]^2+(\mathrm{Re}\Lambda_M)^2}\right\} \quad (14)$$

where the contribution to the absoption centered at $-\omega_0$ has been dropped. In eq 14, Re(z) and Im(z) are the real and imaginary parts of a complex number z and $(\vec{u},\vec{v}) = \Sigma^S_{M=-S+1}u^*_M v_M$ is the hermitian scalar product.

The absorption part of the EPR spectrum at fixed frequency ω and variable field B_0 is proportional to the derivative $d\phi_a^{th}(B_0)/dB_0$ of the absorption function

$$\phi_a^{th}(B_0) = \hat{G}_x(\omega, g\mu_B B_0/\hbar) \quad (15)$$

In this equation, note that Λ_M and $\vec{\eta}_M$, which slightly depend on ω_0, can be approximated by their values at ω. In what follows, the experimental (exp) EPR spectrum, denoted by $d\phi^{exp}(B_0)/dB_0$ includes additive absorption and dispersion contributions. Theoretically, the dispersion contribution $d\phi_d^{th}(B_0)/dB_0$ is derived from the absorption contribution $d\phi_a^{th}(B_0)/dB_0$ using the Kramers−Kronig relation.[22,23]

In the calculation of the spectral densities defined by eq 4 of reference 14

$$j_{MM',M_1M_1'}(\omega) = \int_0^\infty e^{i\omega\tau} \times \overline{\langle M|H_{1S}^{(L)}(t) + H_{1T}^{(L)}(t)|M'\rangle \langle M_1|H_{1S}^{(L)}(t-\tau) + H_{1T}^{(L)}(t-\tau)|M_1'\rangle^*}\, d\tau \quad (16)$$

we find a term involving only the rotation-dependent modulation of the static part of the crystal field described by $H_{1S}^{(L)}(t)$, a pure transient term involving only $H_{1T}^{(L)}$, and cross terms. By assuming that the stochastic fluctuations described by $H_{1T}^{(M)}(t)$ are independent from the rotations, the cross terms vanish. As in reference 14, assuming that the complex undergoes a Brownian rotation with a characteristic time τ_R,

(20) Buckmaster, H. A.; Chatterjee, R.; Shing, Y. H. *Phys. Status Solidi (A)* **1972**, *13*, 9.

we write

$$\tau_k = \frac{\tau_R}{k(k+1)} \tag{17}$$

For the transient part, τ_v denotes the correlation time, and $B_{2\alpha T}(0)$ are the values of the random functions $B_{2\alpha T}(t)$ at $t = 0$ [ref 14, eq 34]. Let τ' be defined by $1/\tau' = 1/\tau_v + 1/\tau_2$ and $\langle S||\mathcal{T}_k||S\rangle$ the reduced matrix elements [ref 14, eq 26]. In analogy to eqs 29 and 36 of reference 14, but now including the imaginary part of the spectral densities, we get:

$$j_{MM',M_1M_1'}(\omega) = \sum_{k=2}^{K} \frac{|\langle S||\mathcal{T}_k||S\rangle|^2}{2k+1}\left(\frac{\tau_k}{1+\omega^2\tau_k^2} + i\frac{\omega\tau_k^2}{1+\omega^2\tau_k^2}\right) \times \tag{18}$$

$$\times \sum_{\alpha} (B_{k\alpha})^2 (-1)^{2S-M-M_1} \begin{pmatrix} S & k & S \\ -M & M-M' & M' \end{pmatrix} \begin{pmatrix} S & k & S \\ -M_1 & M-M' & M_1' \end{pmatrix} +$$

$$+ \frac{|\langle S||\mathcal{T}_2||S\rangle|^2}{5}\left(\frac{\tau'}{1+\omega^2\tau'^2} + i\frac{\omega\tau'^2}{1+\omega^2\tau'^2}\right) \times$$

$$\times \sum_{\alpha} (B_{2\alpha T}(0))^2 (-1)^{2S-M-M_1} \begin{pmatrix} S & 2 & S \\ -M & M-M' & M' \end{pmatrix} \begin{pmatrix} S & 2 & S \\ -M_1 & M-M' & M_1' \end{pmatrix}$$

The imaginary part in eq 18 is at the origin of a small line shift in the spectra called the dynamic shift.[13a,c]

For comparison with experiments we will adjust the following independent parameters defined by

$$a_k := \sqrt{\sum_{\alpha} (B_{k\alpha})^2} \quad \text{and} \quad a_{2T} := \sqrt{\sum_{\alpha} (B_{2\alpha T}(0))^2} \tag{19}$$

It will be assumed that the correlation times have a temperature dependence described by an Arrhenius law ($T_0 = 298.15$ K):[2,3,14]

$$\tau_R(T) = \tau_R(T_0)\, e^{E_R{}^A/R(1/T - 1/T_0)} \tag{20}$$

$$\tau_v(T) = \tau_v(T_0)\, e^{E_v{}^A/R(1/T - 1/T_0)} \tag{21}$$

E_R^A is the activation energy for rotations, E_v^A for the vibrations contained in the transient zero-field splitting. We assume that the complex undergoes a rotational Brownian motion with a diffusion constant D_R which is proportional to T/η in the Stokes−Einstein model, η being the solvent viscosity. Thus, E_R^A is related to $\eta(T)$ through the relation[14]

$$E_R^A = \frac{RT_0T}{T_0 - T} \ln \frac{\eta(T)T_0}{\eta(T_0)T} \tag{22}$$

We summarize the parameters of our model. We have the coefficients a_2, a_4, a_6, and a_{2T}, the characteristic times for rotation $\tau_R(T_0)$ and transient effects $\tau_v(T_0)$ with respective activation energies E_R^A, and E_v^A. We have to add to these parameters the isotropic g-factor allowing the conversion of the values on the abscissa of the spectra from magnetic field into frequency units. Thus, at most nine parameters have to be adjusted in such a way that the theory fits with the existing spectroscopic data. It is worth noting that our model is valid for any symmetry of the static crystal field. Even in the absence of any particular symmetry the number of parameters is not increased, provided that the transient effects are treated only to second order.

3. Computational Details

We built a program which performs a fit of the above parameters to a set of full experimental spectra recorded at multiple frequencies and temperatures. We also developed a program allowing the calculation of the longitudinal relaxation function. Both programs are available from the authors in pure FORTRAN-code. The FORTRAN-code calls freely available subprograms from the EISPACK and MINPACK library.[24]

Now, we consider the fitting procedure in more detail. The measured EPR spectra are a superposition of absorption and dispersion contributions and of a baseline which is a linear function of the magnetic field B_0. For a given set of the nine fitting parameters, the theoretical spectrum is

$$\frac{d\phi^{th}(B_0)}{dB_0} = \xi_1 \frac{d\phi_a^{th}}{dB_0}(B_0) + \xi_2 \frac{d\phi_d^{th}}{dB_0}(B_0) + \xi_3 B_0 + \xi_4 \tag{23}$$

Thus, for each experimental spectrum $d\phi_n^{exp}/dB_0$, where the index n corresponds to a particular temperature and frequency, the associated theoretical spectrum is that given by the parameters ξ_{1n}, ξ_{2n}, ξ_{3n}, ξ_{4n} which minimize the function

$$f_n(\xi_1,\xi_2,\xi_3,\xi_4) = \frac{1}{n_B} \sum_{l=1}^{n_B} \left[\frac{d\phi^{th}}{dB_0}(B_{0,l}) - \frac{d\phi_n^{exp}}{dB_0}(B_{0,l})\right]^2 \tag{24}$$

where n_B is the number of experimental values $B_{0,l}$. All experimental spectra were normalized by the condition

$$\frac{1}{n_B} \sum_{l=1}^{n_B} \left(\frac{d\phi_n^{exp}}{dB_0}(B_{0,l})\right)^2 = 1 \tag{25}$$

to ensure the same weight to each spectrum in the fitting procedure. This provides a set of $4N$ parameters ξ_{in}, $i = 1, ..., 4$, $n = 1, ..., N$, where N is the number of recorded spectra. The nine fitting parameters are adjusted in order to minimize the function

$$F_s = \frac{1}{N} \sum_{n=1}^{N} f_n(\xi_{1n},\xi_{2n},\xi_{3n},\xi_{4n}) \tag{26}$$

Now, we give some technical details about the calculation of the theoretical spectra, the peak-to-peak distances ΔH_{pp}^{th}, and the central fields B_c^{th}. ΔH_{pp}^{th} and B_c^{th} will only be used in a comprehensive comparison of our theoretical results to the experimental counterparts ΔH_{pp}^{exp} and B_c^{exp}, but no fit to these quantities was performed. Since the theoretical line shape is derived from eq 14, we have to diagonalize the relaxation matrix $A^X(-\omega_0)$. This matrix is symmetric with respect to its diagonal and its anti-diagonal.[14] In such a case, it is possible to transform the matrix in block-diagonal form by a similarity transformation with the symmetric matrix T defined by:

$$T_{MM_1} = \frac{1}{\sqrt{2}}(\delta_{-MM_1-1} - \mathrm{sign}(M)\delta_{MM_1} + \sqrt{2}\delta_{MM_1}\delta_{-MM_1-1}),\ M, M_1 = -S+1, ..., S \tag{27}$$

where $\mathrm{sign}(M) = -1$ for $M \le 0$, $\mathrm{sign}(M) = 1$ for $M > 0$. Note that $T^{-1} = T$. The transformed matrix $TA^X(-\omega_0)T$ is reduced to blockdiagonal form with two blocks. But, we must diagonalize the only block for which $\Sigma_{M'} T_{MM'} X_{M'}(0) \neq 0$ so that in

(21) Binsch, G. *Mol. Phys.* **1968**, *15*, 469.
(22) Ayant, Y.; Borg, M. *Fonctions spéciales*; Dunod: Paris, 1971.
(23) Bateman, H. *Tables of Integral Transforms*; Erdelyi, A., Magnus, W., Oberhettinger, F., Tricomi, F. G., Eds.; McGraw-Hill Book Company, Inc.: New York, 1954; Vol. 2.
(24) EISPACK, MINPACK; Netlib Repository, http://www.netlib.org.

eq 14 ($\vec{X}(0),\vec{\eta}_M$) $\neq 0$. This avoids some numerical problems due to the presence of almost degenerate eigenvalues of the matrix $A^X(-\omega_0)$. Although the blocks are not normal matrices, we did not encounter problems of diagonalization in the range of physically reasonable parameters.[5,21]

The central field B_c^{th} and the peak-to-peak distance ΔH_{pp}^{th} were extracted from the expression of the absorption line shape $\phi_a^{th}(B_0)$ by searching the zeros of its first and second derivatives, using the bisection method. There was never any ambiguity in the definition of the peak-to-peak distance to the extent that $d\phi_a^{2th}/dB_0^2$ has only two zeros, because the dynamic shift is small compared to the peak-to-peak distance.

Performance of the programs is in no case a limiting factor since we obtained results within seconds or a few minutes on a personal computer. Of course, the performance depends on the procedure employed in order to minimize eq 26. A good efficiency can be achieved by combining simplex and gradient methods.

4. Results and Discussion

Extensive data[5] are available for full EPR spectra of $[Gd(H_2O)_8]^{3+}$ and $[Gd(DOTA)(H_2O)]^-$ in water at various concentrations at the spectrometer frequencies of 9.425, 75, 150, and 225 GHz, and temperatures between 0 and 100 °C. These experiments are more complete than those used in ref 14 where only the peak-to-peak distances were at the authors' disposal. The published data for $[Gd(DOTA)(H_2O)]^-$ showed an apparent discontinuity in the graph of the central field B_c^{exp} versus temperature at X-band, as well as a lack of experimental points near room temperature. For this reason we performed new X-band (9.425 GHz) measurements of this complex. Solid Na-$[Gd(DOTA)(H_2O)]$ was provided by Guerbet CA, Paris, and used without further purification to prepare a stock solution in bidistilled water. The spectra were recorded on the same Bruker ESP-300 spectrometer as in ref 5.

To minimize the concentration effects on the results of our fitting procedure of the full spectra, we generally took those recorded at the lowest concentration. For $[Gd(DOTA)(H_2O)]^-$ at X-band the new measurements (0.0099 mol/kg) were used instead of the former data (0.005 mol/kg). The concentration effect at X-band is so small that the now higher concentration of $[Gd(DOTA)(H_2O)]^-$ introduces a negligible additional broadening of the spectra.

A significant source of uncertainty in the determination of the model parameters arises from the extraction of the peak-to-peak distances ΔH_{pp}^{exp} and central fields B_c^{exp} which are biased, whatever the extraction method. Indeed, for each experimental spectrum, the associated peak-to-peak distance and apparent *g*-factor are those of a theoretical spectrum of the form (eq 23) which best fits the experiments and obviously corresponds to a particular molecular and line shape model. Such an indirect procedure is necessary because each experimental EPR spectrum is a superposition of absorption and dispersion contributions related to an unknown phasing problem with an additional effect of shifted and tilted baseline.

Until now approximate values of ΔH_{pp}^{exp} and B_c^{exp} were obtained through two different methods. First, a direct reading procedure from the spectra was used, as it was done at X-band in a prior publication,[5] but it is particularly affected by the uncontrollable error due to the lack of knowledge of the phasing of the spectra and of the baseline positions. Second, as done also in ref 5, ΔH_{pp}^{exp} and B_c^{exp} can be determined by fitting a single Lorentzian curve and its corresponding dispersion part to each experimental spectrum to address the phase problem. This implies a monoexponential decay $\exp(-t/T_{2e})$ of the transverse magnetization, clearly being inadequate in sight of our physical relaxation model involving four different exponentials. However, we found that a single Lorentzian line almost perfectly fits the different $[Gd(H_2O)_8]^{3+}$ spectra, whereas the spectra of $[Gd(DOTA)(H_2O)]^-$ are less well reproduced, but the values of T_{2e} do not correspond to a true physical description of the system and are only independent fitted parameters. Nevertheless in this paper, the comparison of peak-to-peak distances and central fields from theory and experiment is a comprehensive way to present our results.[14]

For all of these reasons, in this work, the crystal field parameters, correlation times, activation energies, and *g*-factors were adjusted simultaneously, within our physical model, to the whole set of full, not phase-corrected, spectra as described in the Computational Details section.

In Figure 1, we show some examples of experimental spectra and their counterparts calculated from our best-fitting model for the $[Gd(H_2O)_8]^{3+}$ complex. To summarize the results, we calculated the peak-to-peak distances and central fields of the theoretical absorption spectra and compared them with the data extracted from the experimental spectra used in the fit. In Figure 2, for the convenience of the graphical representation, we do not show the central fields, but we depict the apparent *g*-factor g^{app} which is defined by

$$g^{app} = \frac{\hbar\omega}{\mu_B B_c} \tag{28}$$

where ω is the operating frequency of the spectrometer and B_c the central field.

The displayed "experimental" data points (symbols in Figure 2) differ somewhat from those presented in ref 5 where a different extraction procedure of ΔH_{pp}^{exp} and B_c^{exp} was chosen. The continuous lines are the results for ΔH_{pp}^{th} and B_c^{th} from our model using the parameters shown in Table 1.

4.1. $[Gd(H_2O)_8]^{3+}$. The $[Gd(H_2O)_8]^{3+}$ complex is discussed in more detail because the known square antiprism symmetry of the static crystal field allows a deeper insight in the physics of this complex.

The minimization of the function F_s given by eq 26 with respect to the nine adjustable parameters is rather difficult because of possible mutual compensation effects. We found that the *g*-factor is very well determined at the minimum of F_s whereas it is more difficult to adjust the other parameters. We decided to start from the parameters of model (*iii*) of our previous work[14] limited to the peak-to-peak distance analysis, but fixed the rotational correlation time $\tau_R(T_0)$ at 140 ps and the corresponding activation energy E_R^A at 18.9 kJ/mol in the fitting procedure to maintain them at the values predicted by the Stokes−Einstein model as discussed in ref 14. The parameters of our previous work are recalled in Table 1 in parentheses beside the new adjusted values. The guessed starting value of the *g*-factor was 1.99270. The constraint minimization led to a value $F_{s,min} = 0.013$ of F_s which is somewhat lower than the value 0.038 found for F_s using the initial parameters and the above starting *g* value. The agreement with experimental line shapes, peak-to-peak distances, and dynamic shifts for all of the studied frequencies and temperatures is excellent for the new parameter set as it is demonstrated in Figure 1 for typical examples of whole spectra and in Figure 2a for the peak-to-peak distances and apparent *g*-factors. The line shape is very well reproduced even in the wings of the spectra, underlining the quality of our fit.

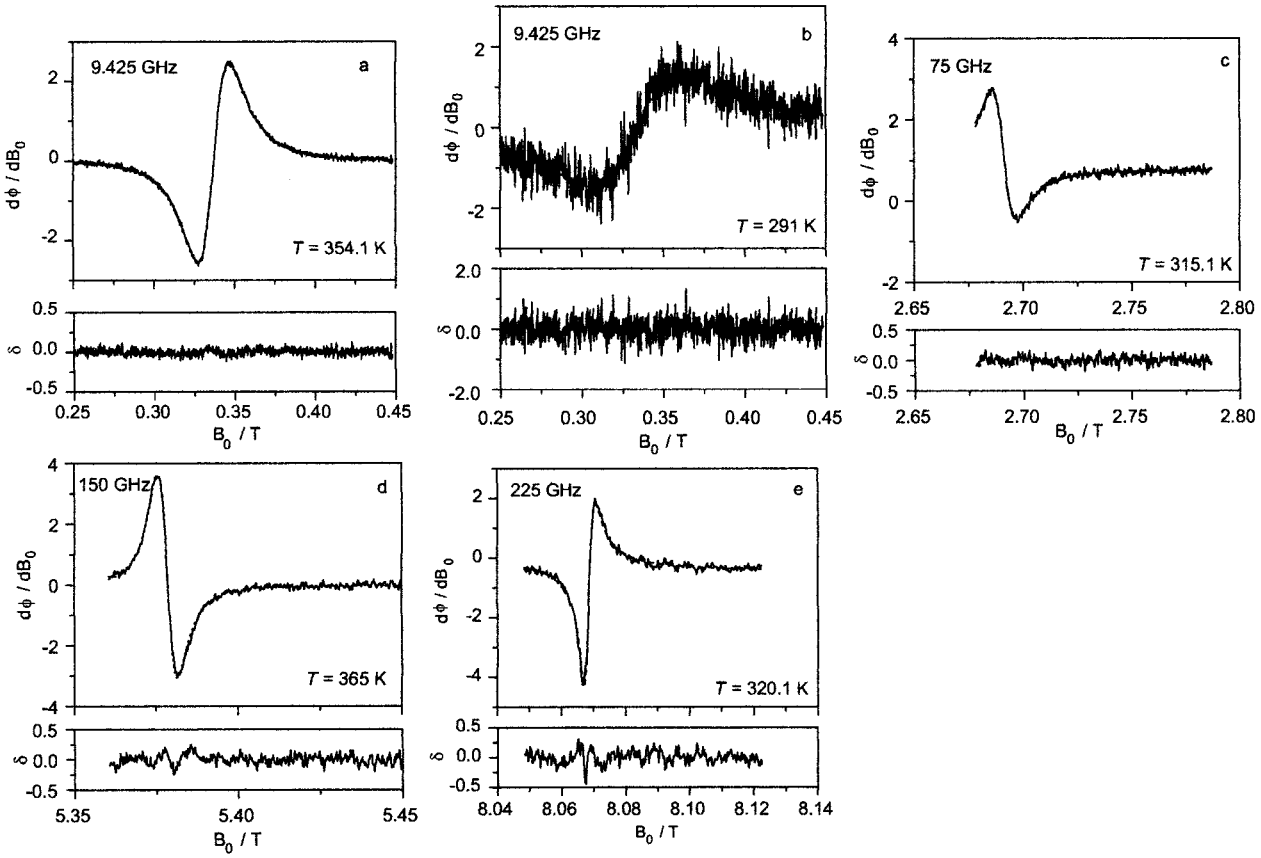

Figure 1. Selected experimental (full line) and nearly identical underlying theoretical spectra (dotted line) for $[Gd(H_2O)_8]^{3+}$ at fixed frequency and temperature versus variable external magnetic field. The theoretical line shape is calculated from the parameters of $[Gd(H_2O)_8]^{3+}$ in Table 1. The difference between experimental and theoretical line shape is shown on the bottom of each figure. (a) 9.425 GHz, 354.0 K; (b) 9.425 GHz, 291.0 K; (c) 75 GHz, 315.1 K; (d) 150GHz, 365.0 K; (e) 225 GHz, 320.1 K.

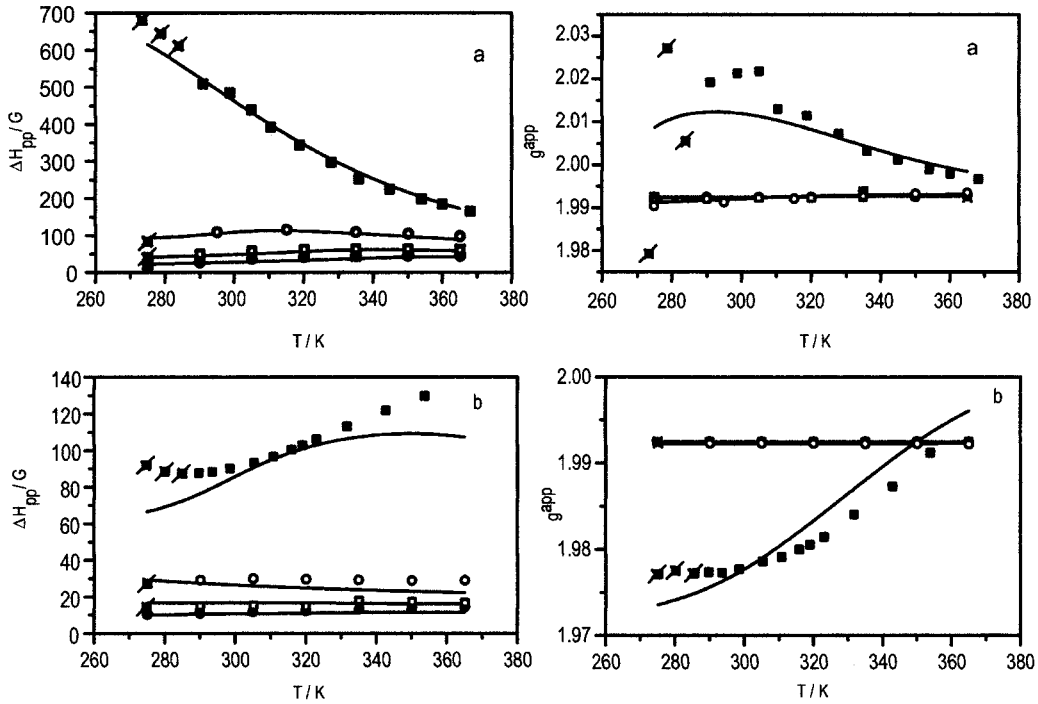

Figure 2. Experimental (symbols) and theoretical (lines) peak-to-peak distances and apparent *g*-factors versus the inverse temperature at different fixed frequencies for (a) $[Gd(H_2O)_8]^{3+}$ and (b) $[Gd(DOTA)(H_2O)]^{-}$ (■) 9.425 GHz (X-band); (○) 75 GHz; (□) 150 GHz; (●) 225 GHz; crossed-out points were not included in the fit (see text).

It should be stressed that it was not necessary to include any contribution from the spin rotation mechanism in our model to interpret the various experiments. This contribution to the transverse relaxation, which is independent of the spectrometer

Table 1. Adjusted Crystal Field and Dynamical Parameters to Yield the Experimental EPR Spectra for the $[Gd(H_2O)_8]^{3+}$ and the $[Gd(DOTA)(H_2O)]^-$ Complex; $F_{s,min}$ Is the Value of the Function (eq 26) F_s at the Local Minimum Given by the Parameter Sets[a]

	$[Gd(H_2O)_8]^{3+}$	$[Gd(DOTA)(H_2O)]^-$
$a_2/(10^{10}\text{rad s}^{-1})$	0.38 (0.29)	0.35
$a_4/(10^{10}\text{rad s}^{-1})$	0.024 (0.023)	–
$a_6/(10^{10}\text{rad s}^{-1})$	0.021 (0.018)	–
$\tau_R(T_0)^{b,c}$/ps	140[d] (190)	491
$E_A^R/(\text{kJ·mol}^{-1})$	18.9[d] (17.7)	16.4
$a_{2T}/(10^{10}\text{rad s}^{-1})$	0.65 (0.74)	0.43
$\tau_v(T_0)^b/(10^{-12}\text{s})$	0.63 (1.1)	0.54
$E_A^v/(\text{kJ·mol}^{-1})$	9.2 (15.0)	6.0[d]
g	1.99273	1.99252
$F_{s,min}$	0.013	0.017

[a] For $[Gd(H_2O)_8]^{3+}$, the eight parameters in parentheses are those from ref 14 and correspond to an adjustement to the sole peak-to-peak distances. [b] $T_0 = 298.15$ K. [c] Note that our $\tau_2 = \tau_R/6$ of eq 17 is often defined as τ_R. [d] Parameter fixed at this value.

frequency, was introduced in other works[3,5] and was leading to an approximate agreement with the experimental data. It does not seem to be effective, a result quite understandable, according to the large size and therefore to the large inertial moment of the magnetic complex.[16] A good agreement with the experiments is possible only with two different, but frequency-dependent crystal field contributions.[14] We observed that the contribution of the static crystal field Hamiltonian is dominant at X-band, but is far less important at higher frequencies.

For the *g*-factor, we found reasonable values comparable to those in other Gd^{3+} salts in solids.[25] The perfect agreement of the experimental spectra with their theoretical counterparts in the framework of our model justifies the choice of $\tau_R(T_0) = 140$ ps and $E_R^A = 18.9$ kJ/mol from the Stokes−Einstein model of rotational diffusion.[14] These values are in reasonable agreement with $\tau_R(T_0) = 6\tau_2(T_0) = 246$ ps and $E_R^A = 15$ kJ/mol given in ref 3 which are deduced from independent NMR experiments (τ_R in ref 3 corresponds to our τ_2).

From the diagonalization of the crystal field Hamiltonian with the square antiprism symmetry of the $[Gd(H_2O)_8]^{3+}$ complex we obtained a total crystal field splitting of the order of 0.46 cm^{-1} whatever the choice of the signs of the coefficients B_2, B_4, B_6. This value is in reasonable agreement with that observed for Gd^{3+} in lanthanum ethyl sulfate (0.25 cm^{-1}) in the solid state.[25] It is not very useful to compare our crystal field parameters a_2 and a_{2T} to the zero-field splitting parameter Δ^2 of previous works,[2,3,5] because Δ^2 reflects an averaged effect of the transient and static zero-field splitting. This is a consequence of the rather simple model including only one second-order term in the Hamiltonian and a unique correlation time to describe all the crystal field fluctuations.

In the context of magnetic resonance imaging, where the Gd^{3+} complexes are used to enhance the longitudinal relaxation rate of the observed water protons, the longitudinal electronic relaxation function $G_z(t)$ plays the major role at the usually applied magnetic fields. This is easily understood in the framework of the modified Solomon−Bloembergen−Morgan approach commonly used to describe the interaction between nuclear and electronic spins.[3,26−28] We observed that $G_z(t)$ is practically a mono-exponential function with a characteristic time T_{1e} having a relative weight of at least 97%, as discussed in ref 14.

4.2. $[Gd(DOTA)(H_2O)]^-$. In the fitting procedure of the whole set of experimental spectra for the $[Gd(DOTA)(H_2O)]^-$ complex we have to be more cautious than in the previous case. The rotation correlation time is longer than for the $[Gd(H_2O)_8]^{3+}$ complex so that the Redfield limit may be violated at low temperatures, mainly for the X-band, as discussed in ref 14. Therefore, the spectra recorded at temperatures lower than 17 °C were not included in the fit. In a first adjustement, we fixed $a_4 = a_6 = 0$ to reduce compensation effects between the parameters. In subsequent adjustements we let freely vary also a_4 and a_6, but their values remained negligible. The lower limit of the activation energy E_v^A was set to 6 kJ/mol. The quality of the adjustment of the spectra is almost as good as for $[Gd(H_2O)_8]^{3+}$ as shown by the similar value of $F_{s,min}$ of F_s. We neglected the fact that the m-$[Gd(DOTA)(H_2O)]^-$ isomer exists in an approximately 4-fold lower quantity besides the M-$[Gd(DOTA)(H_2O)]^-$ isomer (see ref 29) to avoid the introduction of too many parameters. Nevertheless, the agreement with the experiments is good, without any spin rotation mechanism.

The theoretical and experimental values for the peak-to-peak distances and the apparent *g*-factor g^{app} for the $[Gd(DOTA)(H_2O)]^-$ complex are presented in Figure 2b. It must be stressed that the so-called "experimental" peak-to-peak distances and apparent *g*-factors are less well defined as in the case of the aqua complex since the experimental line shapes are no more Lorentzian. The rotational correlation time $\tau_R(T_0) = 491$ ps is very close to that ($6\tau_2(T_0) = 462$ ps) of ref 3. The activation energy for the rotation of the complex is about the same as for the hydrated Gd^{3+} complex. This is expected in the framework of the Stokes−Einstein model for a Brownian rotation in a viscous medium. The rotational correlation time $\tau_R(T_0)$ is roughly proportional to the volumes of the complexes [ref 14, eq 42]. The ratio of the volumes of the $[Gd(DOTA)(H_2O)]^-$ and $[Gd(H_2O)_8]^{3+}$ complexes is estimated from the corresponding Connolly surfaces[30] to be 2.3, while our fits lead to a ratio of 3.5, showing the correct tendency.

In general a full knowledge of the Hamiltonian is not possible without further information because the EPR study does not give access to the coefficients $B_{k\alpha}$ in the static crystal field Hamiltonian (eq 3), but only to the parameters a_k which are the roots of the sums of $B_{k\alpha}^2$ according to eq 19. In the present case, $B_{4\alpha}$ and $B_{6\alpha}$ can be approximated to zero according to the very weak values of a_4 and a_6 obtained with our fitting procedure (see Table 2). The total static crystal field splitting of the $S = {}^7/_2$ multiplet was found to be 0.27 cm^{-1}. For both $[Gd(DOTA)(H_2O)]^-$ isomers, the symmetry group is C_4, leading to three invariant linear combinations, both for $k = 4$ and for $k = 6$. So, we need three coefficients $B_{4\alpha}$, $\alpha = 1, 2, 3$ and three coefficients $B_{6\alpha}$, $\alpha = 1, 2, 3$ to define the static crystal field Hamiltonian.

As for the hydrated Gd^{3+} ion, the adjusted *g*-factor is in reasonable agreement with known *g* values for Gd^{3+} hydrated salts.[25]

5. Conclusions

In this paper, we developed a general method allowing the simultaneous interpretation of the complete EPR line shapes of paramagnetic Gd^{3+} complexes in solution at multiple temper-

(25) Abragam, A.; Bleaney, B. *Electron Paramagnetic Resonance of Transition Ions*; Oxford University Press: New York, 1970; pp 335, 339.
(26) Kowalewski, J.; Nordenskiöld, L.; Benetis, N.; Westlund, P.-O. *Prog. Nucl. Magn. Reson. Spectrosc.* **1985**, *17*, 141.
(27) Vigouroux, C.; Belorizky, E.; Fries, P. H. *Eur. Phys. J. D* **1999**, *5*, 243.
(28) Freed, J. H. *J. Chem. Phys.* **1978**, *68*, 4034.
(29) Aime, S.; Botta, M.; Fasano, M.; Marques, M. P. M.; Geraldes, C. F. G. C.; Pubanz, D.; Merbach, A. E. *Inorg. Chem.* **1997**, *36*, 2059.
(30) Connolly, M. L. *J. Appl. Crystallogr.* **1985**, *16*, 548.

atures and frequencies. In contrast to the approaches used up to now, this model rests on a detailed picture of the crystal field Hamiltonian and of the dynamics of the complex, the parameters of which have all physically meaningful values. We found that it is impossible to determine in a simple way the peak-to-peak distances and central fields from the experimental spectra without the introduction of uncontrollable errors. This is due to a phasing problem of the experimental spectra which cannot be represented by a single Lorentzian. We overcame this problem by a complete line shape analysis. Despite the large amount of spectroscopic data our optimized computer codes yield the model parameters on a modern personal computer within a few minutes. The very good agreement of experimental spectra and their fitted counterparts for $[Gd(H_2O)_8]^{3+}$ and $[Gd(DOTA)(H_2O)]^-$ shows the power of our new approach.

Furthermore, it has been shown that the spin rotation mechanism introduced by other authors,[3,5] plays a negligible role and can be omitted. The introduction of the modulation of all of the terms of the static crystal field by the random rotation of the complex and the effect of the transient zero-field splitting are necessary and sufficient to explain the transverse electronic relaxation of the Gd^{3+} complexes and their EPR spectra. Our model also allows a calculation of the longitudinal electronic relaxation rate relevant in the interpretation of NMR relaxivities.

The line shape calculation is based on Redfield's approximation which may be inadequate in the case of complexes with long rotation correlation times and at very low magnetic fields. It is expected that Redfield's theory is valid if the following two conditions are verified: (i) $|H^{L}_{1}|\tau_c \ll 1$, (ii) $\omega_0 \gg |H^{L}_{1}|^2\tau_c$. As discussed in ref 14, the condition (ii) is always fulfilled in our frequency range. $|H^{L}_{1}|\tau_c$ can be roughly estimated to be $a_2\tau_R(T)/6$ for a temperature T. At $T = 298.15$ K and $T = 274$ K, respectively, the values of $a_2\tau_R(T)/6$ are 0.09 and 0.17 for $[Gd(H_2O)_8]^{3+}$ and 0.29 and 0.5 for $[Gd(DOTA)(H_2O)]^-$ (see Table 1). Consequently, Redfield's theory may be questionable in the description of the experiments at low temperatures. To avoid this problem we excluded the data points below 290 K in our fitting procedure. A more complete analysis of the electronic relaxation beyond the Redfield limit would be of great interest.

Acknowledgment. The authors are grateful to Professor A. Rockenbauer (Hungarian Academy of Sciences, Budapest) for fruitful discussions about the phase problem of the spectra. We are appreciative of the Swiss National Science Foundation and the Office for Education and Science (OFES) for their financial support. This research was carried out in the frame of the EC COST Action D-18 "Lanthanide Chemistry for Diagnosis and Therapy".

Supporting Information Available: Peak-to-peak distances and apparent *g*-factors can be estimated from the experimental EPR spectra as described in the results and discussion section and are given in table S1; a short description of the FORTRAN code employed to fit the whole spectra is given together with an explanation of the accompanying input and output files; a comprehensive overview of the experimental spectra and their fitted counterparts is given in table S2a,b (PDF). This material is available free of charge via the Internet at http://pubs.acs.org.

JA003707U